DALTON
FULL PAPER

Oxidatively induced isomerisation of vinylidene ligands to alkynes: ESR spectra of paramagnetic vinylidene and alkyne arene metal complexes

Ian M. Bartlett,[a] Neil G. Connelly,[a] Antonio J. Martín,[a] A. Guy Orpen,[a] Timothy J. Paget,[a] Anne L. Rieger[b] and Philip H. Rieger[b]

[a] *School of Chemistry, University of Bristol, Bristol, UK BS8 1TS. E-mail: neil.connelly@bristol.ac.uk*
[b] *Department of Chemistry, Brown University, Rhode Island, RI 02912, USA*

Received 3rd December 1998, Accepted 27th January 1999

UV irradiation of $[M(CO)_3(\eta\text{-arene})]$ and $Me_3SiC{\equiv}CSiMe_3$ gives $[M(CO)_2\{C{=}C(SiMe_3)_2\}(\eta\text{-arene})]$ (M = Cr, arene = $C_6H_2Me_4$-1,2,3,5 **2V**, $C_6H_3Me_3$-1,2,3 **3V** or C_6H_6 **4V**; M = Mo, arene = C_6Me_6 **5V** or $C_6H_3Me_3$-1,3,5 **6V**). The crystal structure of $[Cr(CO)_2\{C{=}C(SiMe_3)_2\}(\eta\text{-}C_6H_6)]$ **4V** confirms the presence of the vinylidene ligand; the complex has approximate C_s symmetry with the $C(SiMe_3)_2$ plane orthogonal to the $arene_{centroid}$–Cr–C_α–C_β plane. Voltammetry and IR and NMR spectroscopy show that in solution $[Mo(CO)_2\{C{=}C(SiMe_3)_2\}(\eta\text{-}C_6H_3Me_3\text{-}1,3,5)]$ **6V** thermally equilibrates with the alkyne isomer $[Mo(CO)_2(\eta\text{-}Me_3SiC{\equiv}CSiMe_3)(\eta\text{-}C_6H_3Me_3\text{-}1,3,5)]$ **6A**. The vinylidene complexes $[M(CO)_2\{C{=}C(SiMe_3)_2\}(\eta\text{-arene})]$ **2V**–**6V** undergo one-electron oxidation to the alkyne cations $[M(CO)_2(\eta\text{-}Me_3SiC{\equiv}CSiMe_3)(\eta\text{-arene})]^+$ **2A**$^+$–**6A**$^+$ *via* fast, redox-induced vinylidene-to-alkyne isomerisation. These cations are reduced to the neutral alkyne complexes $[M(CO)_2(\eta\text{-}Me_3SiC{\equiv}CSiMe_3)(\eta\text{-arene})]$ **2A**–**6A** which slowly isomerise thermally to the neutral vinylidene complexes **2V**–**6V**. Paramagnetic vinylidene and alkyne complex cations have been characterised by ESR spectroscopy; unpaired electron density is extensively delocalised from the metal centre to the C_2 ligand, in agreement with the results of EHMO calculations.

Introduction

We have recently presented[1] the results of a detailed study of the mechanism of the redox-induced isomerisation processes linking the vinylidene complex $[Cr(CO)_2\{C{=}C(SiMe_3)_2\}(\eta\text{-}C_6Me_6)]$ **1V** with the alkyne cation $[Cr(CO)_2(\eta\text{-}Me_3SiC{\equiv}CSiMe_3)(\eta\text{-}C_6Me_6)]^+$ **1A**$^+$, quantifying the kinetics of the conversion of **1V**$^+$ into **1A**$^+$ and of **1A** into **1V**. We have also noted that related alkyne cations $[Cr(CO)_2(\eta\text{-}RC{\equiv}CR)(\eta\text{-}C_6Me_6)]^+$ (R = Ph, C_6H_4OMe-4, *etc.*) can be made directly from the neutral complexes $[Cr(CO)_2(\eta\text{-}RC{\equiv}CR)(\eta\text{-}C_6Me_6)]$,[2,3] and have made a brief comparison of the structures of the redox-related pair $[Cr(CO)_2(\eta\text{-}PhC{\equiv}CPh)(\eta\text{-}C_6Me_5H)]^z$ (z = 0 or 1).[4] We now describe the characterisation of a wider series of vinylidene complexes, $[M(CO)_2\{C{=}C(SiMe_3)_2\}(\eta\text{-arene})]$ (M = Cr, arene = $C_6H_2Me_4$-1,2,3,5 **2V**, $C_6H_3Me_3$-1,2,3 **3V** or C_6H_6 **4V**; M = Mo, arene = C_6Me_6 **5V** or $C_6H_3Me_3$-1,3,5 **6V**), including the crystal structure of $[Cr(CO)_2\{C{=}C(SiMe_3)_2\}(\eta\text{-}C_6H_6)]$ **4V**, and their oxidative isomerisation to the corresponding alkyne cations. Moreover, ESR spectroscopic analysis and EHMO calculations have provided insight into the electronic structure of a unique set of paramagnetic vinylidene and alkyne complex isomers.

Results and discussion

Synthesis of $[M(CO)_2\{C{=}C(SiMe_3)_2\}(\eta\text{-arene})]$ (M = Cr or Mo)

The chromium and molybdenum complexes $[M(CO)_2\{C{=}C(SiMe_3)_2\}(\eta\text{-arene})]$ [M = Cr, arene = $C_6H_2Me_4$-1,2,3,5 **2V**, $C_6H_3Me_3$-1,2,3 **3V** or C_6H_6 **4V**; M = Mo, arene = C_6Me_6 **5V** or $C_6H_3Me_3$-1,3,5 **6V**) (Chart 1) were prepared by a method analogous to that previously described[1] for $[Cr(CO)_2\{C{=}C(SiMe_3)_2\}(\eta\text{-}C_6Me_6)]$ **1V**, namely by the UV irradiation of a mixture of $[M(CO)_3(\eta\text{-arene})]$ and $Me_3SiC{\equiv}CSiMe_3$ in solution; the tungsten complexes $[W(CO)_3(\eta\text{-arene})]$ (arene = $C_6H_3Me_3$-1,3,5 and C_6Me_6) did not react with $Me_3SiC{\equiv}CSiMe_3$ under the same conditions.

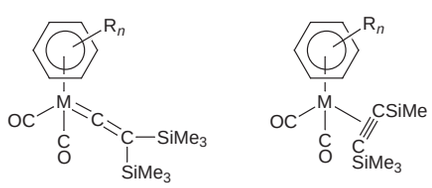

V **A**

Complex	M	R_n
1V/1A	Cr	Me_6
2V/2A	Cr	H_2Me_4–1,2,3,5
3V/3A	Cr	H_3Me_3–1,2,3
4V/4A	Cr	H_6
5V/5A	Mo	Me_6
6V/6A	Mo	H_3Me_3–1,3,5

Chart 1 Numbering of vinylidene and alkyne complexes.

The solvent used for the photolysis reaction influences both the yield and reaction time. Thus, complex **2V** was prepared in good yield by irradiation in thf whereas the use of this solvent for the less stable complexes **3V**, **4V** and **6V** resulted in extensive decomposition and *n*-hexane was found to give higher yields. The molybdenum complex $[Mo(CO)_3(\eta\text{-}C_6Me_6)]$ reacted very slowly with $Me_3SiC{\equiv}CSiMe_3$ in *n*-hexane or thf (*ca.* 10% conversion in thf after 15 h) but the reaction rate was significantly increased in benzene or toluene (*ca.* 70% conversion in benzene after 15 h). During the preparation of the vinylidene complex $[Mo(CO)_2\{C{=}C(SiMe_3)_2\}(\eta\text{-}C_6H_3Me_3\text{-}1,3,5)]$ **6V** the formation of a second product, shown below to be the alkyne isomer $[Mo(CO)_2(\eta\text{-}Me_3SiC{\equiv}CSiMe_3)(\eta\text{-}C_6H_3Me_3\text{-}1,3,5)]$ **6A**, was observed; pure samples of **6V** were, however, isolated by slow crystallisation from *n*-hexane at −20 °C.

Table 1 Analytical, electrochemical and IR spectroscopic data for chromium and molybdenum arene vinylidene complexes

Complex	Colour	Yield (%)	Analysis[a] (%)		IR[b]/cm^{-1}		
			C	H	ν(CO)	ν(C=C)	$E^{c,d}$/V
$[Cr(CO)_2\{C{=}C(SiMe_3)_2\}(\eta\text{-}C_6Me_6)]$[e] **1V**	Orange	—	—	—	1925, 1872ms	1567m	0.18 (−0.24)
$[Cr(CO)_2\{C{=}C(SiMe_3)_2\}(\eta\text{-}C_6H_2Me_4\text{-}1,2,3,5)]$ **2V**	Orange	39	58.3 (58.2)	7.7 (7.8)	1933, 1881ms 1913, 1849ms[d]	1576m 1575[d]	0.25 (−0.13)
$[Cr(CO)_2\{C{=}C(SiMe_3)_2\}(\eta\text{-}C_6H_3Me_3\text{-}1,2,3)]$ **3V**	Orange	38	57.4 (57.3)	7.8 (7.6)	1937, 1886ms 1918, 1855ms[d]	1576m 1576[d]	0.28 (−0.13)
$[Cr(CO)_2\{C{=}C(SiMe_3)_2\}(\eta\text{-}C_6H_6)]$ **4V**	Red	22	54.0 (53.9)	7.2 (6.8)	1949, 1900ms 1929, 1869ms[d]	1586m 1585[d]	0.34 (−0.03)
$[Mo(CO)_2\{C{=}C(SiMe_3)_2\}(\eta\text{-}C_6Me_6)]$ **5V**	Orange	27	54.5 (54.5)	7.5 (7.5)	1928, 1871ms 1905, 1834ms[d]	1567m 1566[d]	0.35 (−0.01)
$[Mo(CO)_2\{C{=}C(SiMe_3)_2\}(\eta\text{-}C_6H_3Me_3\text{-}1,3,5)]$ **6V**	Orange-red	19	51.3 (51.6)	6.9 (6.9)	1940, 1884ms 1917, 1848ms[d] 1915w, 1851w[f] 1898w, 1818w[f,d]	1578m 1578[d] — —	0.44 (0.13)

[a] Calculated values in parentheses. [b] Strong (s) absorptions in *n*-hexane unless otherwise stated, m = medium, w = weak. [c] Peak potential, E_{pk}, of the irreversible oxidation wave; potential for the reversible product wave in parentheses. [d] In CH_2Cl_2. [e] From ref. 1. [f] Bands for the isomeric alkyne complex $[Mo(CO)_2(\eta\text{-}Me_3SiC{\equiv}CSiMe_3)(\eta\text{-}C_6H_3Me_3\text{-}1,3,5)]$ **6A**.

Table 2 Proton and $^{13}C\text{-}\{^1H\}$ NMR spectroscopic data for arene chromium and molybdenum complexes[a]

Compound	^{1}H	$^{13}C\text{-}\{^1H\}$
2V	0.35 (18H, s, SiMe_3), 1.60 (3H, s, Me[2] or Me[5]), 1.75 (3H, s, Me[2] or Me[5]), 1.78 (6H, s, Me[1,3]), 4.55 (2H, s, H[4,6])	2.7 (SiMe_3), 14.7 (Me[5]), 19.6 (Me[1,3]), 19.8 (Me[2]), 98.5 (*C*H[4,6]), 105.7 (C_β), 107.7 (*C*Me[5]), 110.8 (*C*Me[2]), 112.4 (*C*Me[1,3]), 239.5 (CO), 349.2 (C_α)
3V	0.38 (18H, s, SiMe_3), 1.63 (3H, s, Me[2]), 1.77 (6H, s, Me[1,3]), 4.65 (2H, d, JH[4]H[5] and JH[5]H[6] 6, H[4,6]), 4.75 (1H, t, JH[4]H[5] and JH[5]H[6] 6, H[5])	2.6 (SiMe_3), 14.9 (Me[2]), 19.6 (Me[1,3]), 96.6 (*C*H[5]), 97.2 (*C*H[4,6]), 106.4 (C_β), 110.1 (*C*Me[2]), 112.0 (*C*Me[1,3]), 239.3 (CO), 348.3 (C_α)
4V	0.36 (18H, s, SiMe_3), 4.66 (6H, s, C_6H_6)	2.2 (SiMe_3), 96.0 (C_6H_6), 107.7 (C_β), 238.7 (CO), 347.5 (C_α)
5V	0.41 (18H, s, SiMe_3), 1.89 (18H, s, C_6Me_6)	2.4 (SiMe_3), 17.8 (C*Me*), 101.8 (C_β), 114.2 (*C*Me), 231.4 (CO), 331.8 (C_α)[b]
6V	0.39 (18H, s, SiMe_3), 1.79 (9H, s, C*Me*), 4.79 (3H, s, C*H*)	2.5 (SiMe_3), 20.5 (C*Me*), 98.8 (*C*H), 100.2 (C_β), 116.4 (*C*Me), 229.4 (CO), 333.4 (C_α)
6A	0.41 (18H, s, SiMe_3), 1.71 (9H, s, C*Me*), 4.68 (3H, s, C*H*)	1.7 (SiMe_3), 20.2 (C*Me*), 93.5 (*C*H), 107.1 (*C*SiMe_3), 110.1 (*C*Me), 237.4 (CO)

[a] Chemical shift (δ) in ppm, J values in Hz, spectra in C_6D_6 unless stated otherwise. [b] In $CDCl_3$.

There is an extensive array of complexes of the type $[Cr(CO)_2L(\eta\text{-arene})]$ (*e.g.* L = PR_3, RC≡CR, $R_2C{=}CR_2$, RCN, py, CS, N_2, thf, *etc.*),[5] but **5V** and **6V** are rare examples of the molybdenum analogues $[Mo(CO)_2L(\eta\text{-arene})]$. Generally, carbonyl substitution does not occur when $[Mo(CO)_3(\eta\text{-arene})]$ is treated with L, either thermally or photochemically, mainly because the Mo–C_{arene} bonds are easily cleaved. Indeed, replacement of the arene in $[Mo(CO)_3(\eta\text{-arene})]$ by L provides a convenient and general route to *fac*-$[Mo(CO)_3L_3]$.[6]

Characterisation of the vinylidene complexes 2V–6V

Complexes **2V**–**6V** are orange to red crystalline solids the air stability of which decreases from chromium to molybdenum and with decreasing substitution at the arene; solutions of **4V** and **6V** decompose in air over several minutes. The complexes were characterised by elemental analysis and by IR (Table 1) and NMR spectroscopy (Table 2). The IR spectra show two strong carbonyl bands (between 1834 and 1949 cm^{-1}) and a third, weaker, band at lower energy (1566 to 1586 cm^{-1}); the last is assigned to ν(C=C) and is typical of a vinylidene complex.[7] Both ν(CO) and ν(C=C) for **1V**–**6V** move to lower energy as methylation at the arene is increased although changing the metal from Cr to Mo has little effect. Increased methylation causes the arene to become a better electron donor so that back donation from M to π* CO and $C{=}CR_2$ orbitals increases. The vinylidene ligand is generally considered to be a good, essentially single-faced π-acceptor[8] and the vinylidene ligand of $[Mn(CO)_2(C{=}CHPh)(\eta\text{-}C_5H_5)]$ has been classified as a better π acceptor than CO.[9]

The carbonyl bands of **1V**–**6V** are considerably lower in energy than those of $[Cr(CO)_2(C{=}CR_2)(\eta\text{-arene})]$ (R = Me or Ph)[10] (*e.g.* 1980 and 1930 cm^{-1} for $[Cr(CO)_2(C{=}CPh_2)(\eta\text{-}C_6H_6)]$). Thus the π-accepting ability of the vinylidene ligands follows the order: $C{=}CPh_2 > C{=}CMe_2 \gg C{=}C(SiMe_3)_2$. Since β-silyl groups can stabilise carbocations,[11] this stabilising effect may also decrease the electrophilicity of C_α of the vinylidene, so reducing the acceptor ability of the ligand.

Uniquely, the IR spectrum of pure **6V** in CH_2Cl_2 changed with time, two extra bands appearing at 1898 and 1818 cm^{-1}. These bands continued to grow for *ca.* 1 h at which point equilibrium appeared to be reached (see below). The new bands are lower in energy than those of **6V** (1917, 1848 cm^{-1}), consistent with the formation of the alkyne isomer $[Mo(CO)_2(\eta\text{-}Me_3SiC{\equiv}CSiMe_3)(\eta\text{-}C_6H_3Me_3)]$ **6A**. A similar difference was noted[1] between the bands of $[Cr(CO)_2\{C{=}C(SiMe_3)_2\}(\eta\text{-}C_6Me_6)]$ **1V** (1901, 1834 cm^{-1}) and those of $[Cr(CO)_2(\eta\text{-}Me_3SiC{\equiv}CSiMe_3)(\eta\text{-}C_6Me_6)]$ (**1A**) (1874 and 1799 cm^{-1}).

NMR spectroscopy

The ^{1}H NMR spectra of **2V**–**6V** (Table 2) do not allow a distinction to be made between the presence of vinylidene or alkyne ligands. Each complex shows a single resonance for the methyl protons of the $SiMe_3$ groups and the expected signals for the arene protons and methyl substituents. However, the different C_2 ligands can be distinguished by the characteristic $^{13}C\text{-}\{^1H\}$ NMR resonances of the vinylidene fragment. Thus C_α, the highly deshielded carbon atom bonded directly to the metal, is typically observed between δ 258 and 382[7] whereas C_β, much less deshielded, is typically observed between δ 87 and 143. For the chromium complexes **2V**–**4V** C_α appears as a weak

Table 3 Selected bond lengths (Å) and angles (°) for $[Cr(CO)_2\{C{=}C(SiMe_3)_2\}(\eta\text{-}C_6H_6)]$ **4V**

Cr–C(1)	2.229(6)	Cr–C(7)	1.837(7)
Cr–C(2)	2.204(7)	Cr–C(8)	1.838(9)
Cr–C(3)	2.206(8)	ave. Cr–CO	1.838(9)
Cr–C(4)	2.230(8)		
Cr–C(5)	2.215(7)	Cr–C(9)	1.854(5)
Cr–C(6)	2.228(6)	C(9)–C(10)	1.297(7)
ave. $Cr–C_{arene}$ [a]	2.216(8)		
		C(10)–Si(1)	1.872(5)
Si(1)–C(11)	1.848(7)	C(10)–Si(2)	1.883(5)
Si(1)–C(12)	1.854(7)	ave. C(10)–Si(Me)	1.878(5)
Si(1)–C(13)	1.834(9)		
Si(2)–C(14)	1.832(8)	C(7)–O(1)	1.155(7)
Si(2)–C(15)	1.814(11)	C(8)–O(2)	1.145(8)
Si(2)–C(16)	1.810(10)		
Cr–C(9)–C(10)	176.5(4)	Si(1)–C(10)–Si(2)	123.6(3)
C(9)–C(10)–Si(1)	119.3(4)	C(7)–Cr–C(8)	85.9(3)
C(9)–C(10)–Si(2)	117.1(4)	C(7)–Cr–C(9)	90.5(3)
Cr–C(7)–O(1)	179.5(7)	C(8)–Cr–C(9)	86.2(3)
Cr–C(8)–O(2)	177.1(6)		

[a] The error given for the mean values is the largest individual standard deviation in the set of values averaged.

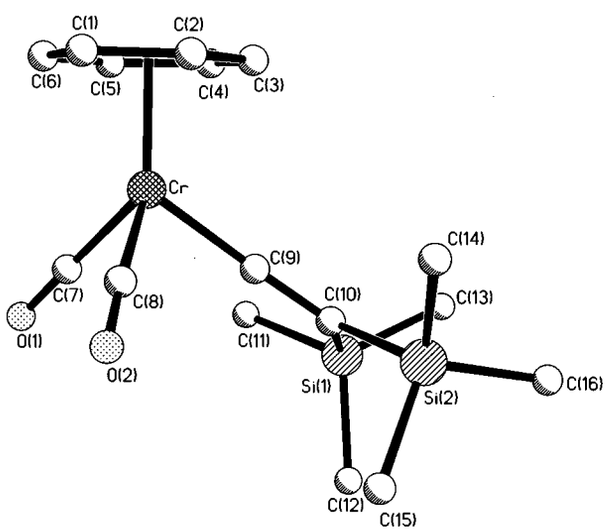

Fig. 1 The molecular structure of $[Cr(CO)_2\{C{=}C(SiMe_3)_2\}(\eta\text{-}C_6H_6)]$ **4V** showing the atom labelling scheme. Hydrogen atoms have been omitted for clarity.

resonance between δ 347 and 350; in the molybdenum complexes **5V** and **6V**, C_α is slightly less deshielded, at δ 332 and 334 respectively. The signal for C_β is also very weak but is observed between δ 105 and 108 in **2V**–**4V** and at δ 102 and 100 in **5V** and **6V** respectively. Similar shifts for C_α and C_β were reported for $[Cr(CO)_2(C{=}CR_2)(\eta\text{-}C_6H_6)]$; C_α is at δ 313 (R = Me) and 328 (R = Ph), and C_β is at δ 134 (R = Me) and 132 (R = Ph).[10]

The room temperature ^1H and $^{13}C\text{-}\{^1H\}$ NMR spectra of **6V** also show the presence of the alkyne isomer $[Mo(CO)_2(\eta\text{-}Me_3SiC{\equiv}CSiMe_3)(\eta\text{-}C_6H_3Me_3)]$ **6A** (Table 2); integration of the alkyne and vinylidene peaks in the ^1H spectrum provides an estimated ratio of 5:1 for the vinylidene to alkyne isomers.

The crystal structure of $[Cr(CO)_2\{C{=}C(SiMe_3)_2\}(\eta\text{-}C_6H_6)]$ 4V

The ^{13}C NMR and IR spectra provide strong evidence for the formulation of **1V**–**6V** as vinylidene complexes. However, the crystal structure of **4V** was determined in order to verify the structure and compare the structural parameters with those of other vinylidene complexes.

Crystals of $[Cr(CO)_2\{C{=}C(SiMe_3)_2\}(\eta\text{-}C_6H_6)]$ **4V** were grown from a concentrated *n*-hexane solution cooled to −20 °C for 16 h. The molecular structure of **4V** is shown in Fig. 1 and important bond lengths and angles are listed in Table 3. The benzene ligand effectively occupies three co-ordination sites of a pseudo-octahedral geometry; the $Cr–C_{arene}$ distances are in the range 2.204–2.230 Å. The metal–carbonyl angles are essentially linear and the Cr–C(O) lengths [average 1.838(9) Å] are similar to those of other neutral arene chromium complexes such as $[Cr(CO)_3(\eta\text{-}C_6H_6)]$ (1.844 Å).[12] The almost linear Cr–C(9)–C(10) angle [176.5(4)°] and the short distances Cr–C(9) [1.854(5) Å] and C(9)–C(10) [1.297(7) Å] are consistent with the presence of metal–carbon and carbon–carbon double bonds, as observed in other vinylidene complexes.[7] The geometry around C(10) (C_β) is essentially trigonal (angles 117.1–123.6°), consistent with sp^2 hybridisation. The large size of the $SiMe_3$ group is reflected in the Si(1)–C(10)–Si(2) angle [123.6(3)°].

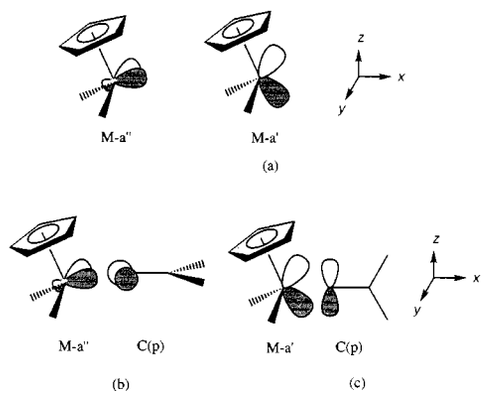

Fig. 2 (a) Important orbitals of the $M(CO)_2(\eta\text{-}C_5H_5)$ fragment; (b) horizontal and (c) vertical orientations for complexes $[M(CO)_2(C{=}CR_2)(\eta\text{-}C_5H_5)]^z$ (M = Mn, z = 0; M = Fe, z = 1).

The silyl atoms of the $SiMe_3$ substituents of the vinylidene ligand lie in a plane perpendicular to an approximate mirror plane lying through AR–Cr–C_α-C_β (AR = centre of the arene), the orientation observed for the isoelectronic complex $[Mn(CO)_2(C{=}CMe_2)(\eta\text{-}C_5H_5)]$.[13] Molecular orbital studies on $[Mn(CO)_2(C{=}CR_2)(\eta\text{-}C_5H_5)]$ have been carried out by Hoffmann[14] and Fenske.[15] The valence orbitals in the metal fragment $[Mn(CO)_2(\eta\text{-}C_5H_5)]$ are derived from those of $[Mn(CO)_3(\eta\text{-}C_5H_5)]$; the two most important orbitals involved in bonding to the vinylidene ligand are shown in Fig. 2a. Two symmetrical orientations are possible for the vinylidene, coinciding with the symmetry plane (vertical, the *xz* plane in Fig. 2b) or bisecting the symmetry plane (horizontal, the *yz* plane in Fig. 2c). In the horizontal orientation the π and π* orbitals on the vinylidene interact with the metal-based orbitals of a′ symmetry, and the vacant vinylidene C(p) orbital interacts with the metal orbitals of a″ symmetry. In the vertical orientation the combinations are reversed. Thus, the C–C π and π* orbitals overlap with the metal orbitals a″ and the C(p) orbital overlaps with the metal a′ orbitals. For the complexes $[M(CO)_2(C{=}CR_2)(\eta\text{-}C_5H_5)]^{z+}$ (M = Fe, z = 1; M = Mn, z = 0) the interaction of the p orbital on C_α with the metal a″ orbital sets the ground state orientation as horizontal (Fig. 2a). However, this orientation is only marginally lower in energy than the vertical orientation and the energy barrier to rotation of the vinylidene ligand is *ca.* 17 kJ mol^{-1} for $[Mn(CO)_2(C{=}CR_2)(\eta\text{-}C_5H_5)]$.[15] The horizontal orientation appears to be similarly favoured in the arenechromium complex **4V**.

Electrochemistry

The CVs of **2V**–**6V**, at a platinum electrode in CH_2Cl_2 and at a scan rate of 200 mV s^{-1}, are similar to that of **1V**,[1] showing an irreversible oxidation wave, in the range 0.18 to 0.44 V, (Table 1) accompanied by a reversible product wave, between −0.24 and 0.13 V. Decreasing methylation of the arene increases the potential of both the irreversible oxidation wave and the

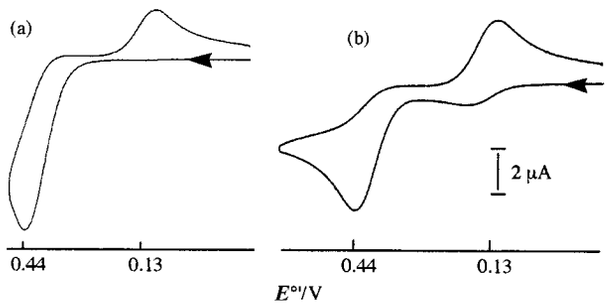

Fig. 3 CV of $[Mo(CO)_2\{C{=}C(SiMe_3)_2\}(\eta\text{-}C_6H_3Me_3\text{-}1,3,5)]$ **6V**, (a) after *ca.* 30 s, (b) after 20 min.

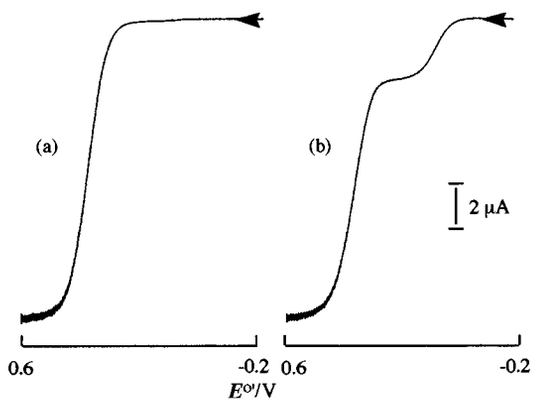

Fig. 4 Voltammograms of $[Mo(CO)_2\{C{=}C(SiMe_3)_2\}(\eta\text{-}C_6H_3Me_3\text{-}1,3,5)]$ **6V**, from −0.2 to 0.6 V, at a rotating platinum electrode (a) after 45 s, (b) after 2 h.

reversible product wave, by *ca.* 30 mV per methyl substituent, reflecting the reduced electron density at the metal. The molybdenum complexes are significantly more difficult to oxidise than their chromium analogues (by *ca.* 170 mV).

The irreversible oxidation wave corresponds to the formation of the cationic vinylidene complex $[M(CO)_2\{C{=}C(SiMe_3)_2\}(\eta\text{-arene})]^+$ and its isomerisation to the cationic alkyne complex $[M(CO)_2(\eta\text{-}Me_3SiC{\equiv}CSiMe_3)(\eta\text{-arene})]^+$. That the product wave is reversible shows that the isomerisation of $[M(CO)_2(\eta\text{-}Me_3SiC{\equiv}CSiMe_3)(\eta\text{-arene})]$ to $[M(CO)_2\{C{=}C(SiMe_3)_2\}(\eta\text{-arene})]$ is slow on the CV timescale. The more positive potential for the oxidation of the vinylidene complex (*cf.* that for the alkyne complex) reflects a more electron-deficient metal centre.

As noted above, NMR and IR spectroscopy suggested that the vinylidene complex $[Mo(CO)_2\{C{=}C(SiMe_3)_2\}(\eta\text{-}C_6H_3Me_3\text{-}1,3,5)]$ **6V** slowly equilibrates with the alkyne isomer $[Mo(CO)_2(\eta\text{-}Me_3SiC{\equiv}CSiMe_3)(\eta\text{-}C_6H_3Me_3\text{-}1,3,5)]$ **6A**. The voltammetry of **6V** provides conclusive evidence that *thermally* induced vinylidene-to-alkyne isomerisation does occur in solution (as well as the oxidatively-induced isomerisation process). Fig. 3a shows the CV of **6V** ran immediately following the addition of a pure solid sample to the electrochemical cell; it is similar to those observed for the other vinylidene complexes **2V**–**5V**. However, over *ca.* 20 min a second oxidation wave appears at a potential associated with the oxidation wave of the alkyne complex **6A** (Fig. 3b). At this point the IR spectrum of the solution in the electrochemical cell showed the two new bands, at 1898 and 1818 cm^{-1}, assigned to the alkyne isomer.

The formation with time of the alkyne complex **6A** was also studied by using a rotating platinum electrode. Fig. 4a shows the rotating platinum electrode voltammogram (rpev) *ca.* 45 s after adding **6V** to the electrochemical cell; there is only one wave, corresponding to the oxidation of the vinylidene complex. After 5 min a second wave, at the potential anticipated for the alkyne complex **6A**, begins to appear; Fig. 4b shows the rpev after 2 h by which time equilibrium had been reached. The relative wave heights provide an estimated vinylidene : alkyne ratio at equilibrium of 5 : 1, in good agreement with the results of ^1H NMR spectroscopy.

Table 4 IR spectroscopic and electrochemical data for alkyne complexes

	IR [a]/cm^{-1}		
Complex	ν(CO)	ν(C≡C)	$E^{o\prime}$/V
1A [b]	1874, 1799ms	—	−0.24 [c]
1A$^+$ [b]	2015ms, 1950	1764w	
2A	1891, 1817ms	—	−0.13 [c]
2A$^+$	2027ms, 1961	1785w	
3A	1898, 1826ms	—	−0.13 [c]
3A$^+$	2040ms, 1959	1791w	
4A	1911, 1841ms	—	−0.03 [c]
4A$^+$	2046ms, 1981	1810w	
5A	1879, 1802ms	—	−0.01 [c]
5A$^+$	2001, 1941	1736w	
6A	1898, 1818	—	0.13 [c]
6A$^+$	2013, 1957	—	
7A [d]	1937, 1861	—	0.12
7A$^+$	2060, 2010	—	
8A [d]	1889, 1811	—	−0.24, 0.89
8A$^+$	2011, 1965	—	
9A [d]	1894, 1821	—	−0.18
9A$^+$	2034, 1976	—	

[a] Strong absorptions (s) in CH_2Cl_2 unless otherwise stated, m = medium, w = weak. [b] From ref. 1. [c] Potential data taken from the reversible product wave observed in the cyclic voltammogram of the isomeric vinylidene complex, in CH_2Cl_2. [d] $[Cr(CO)_2(\eta\text{-}RC{\equiv}CR')(\eta\text{-}C_6Me_6)]$ R = R′ = O_2CEt **7A**, R = R′ = C_6H_4OMe-4 **8A**, R = Ph, R′ = H **9A**.

For the majority of alkyne and vinylidene complexes, the *inter*conversion of the two bonding modes of the C_2 fragment is not observed although in some syntheses of vinylidene complexes from terminal alkynes and a d^6 metal centre an intermediate alkyne complex has been detected.[16,17] Where isomerisation has been reported, alkyne-to-vinylidene rearrangements are far more common than the reverse vinylidene-to-alkyne isomerisation and the equilibrium between alkyne and vinylidene usually favours one isomer outright. However, the terminal alkyne complex $[Re(PPh_3)(\eta\text{-}Bu^tC{\equiv}CH)(NO)(\eta\text{-}C_5H_5)]^+$, when heated to 80 °C for 2 h, undergoes alkyne-to-vinylidene isomerisation to give mostly $[Re(PPh_3)(C{=}CHBu^t)(NO)(\eta\text{-}C_5H_5)]^+$; a small amount (*ca.* 14% by ^1H NMR spectroscopy) of $[Re(PPh_3)(\eta\text{-}Bu^tC{\equiv}CH)(NO)(\eta\text{-}C_5H_5)]^+$ remained even after 7 h. The vinylidene complex $[Re(PPh_3)(C{=}CHBu^t)(NO)(\eta\text{-}C_5H_5)]^+$ has also been made by protonating the alkynyl complex $[Re(PPh_3)(C{\equiv}CBu^t)(NO)(\eta\text{-}C_5H_5)]$ with $H[BF_4]$ at −78 °C where no alkyne complex is formed. However, heating this cation to 80 °C for 2 h resulted in the same ratio of vinylidene and alkyne isomers, confirming that thermal equilibrium occurs at 80 °C.[18]

The vinylidene complexes **2V**–**6V** are favoured over the alkyne complexes **2A**–**6A** in that the repulsive interactions between the t_{2g} orbitals (assuming octahedral symmetry) of the d^6 metal and the filled alkyne $\pi_\perp$ orbital are alleviated. Given the (unique) thermal isomerisation of **6V** to **6A**, the repulsive interaction appears to be alleviated by reducing the number of methyl groups on the arene and by replacing chromium by molybdenum.

Chemical redox reactions

The chemical oxidation of **2V**–**4V** was readily effected by adding one equivalent of $[Fe(\eta\text{-}C_5H_5)_2][PF_6]$ to a CH_2Cl_2 solution of the chromium complexes at 0 °C. In each case, the IR spectrum of the resulting yellow solution shows two new carbonyl

bands shifted to higher energy (by *ca.* 90 cm^{-1}) (Table 4), consistent with the formation of a cationic complex. Furthermore, as in the oxidation of **1V**, the ν(C=C) band in **2V**–**4V** is replaced by a much weaker band at higher energy (1785 to 1810 cm^{-1}) assigned to ν(C≡C), indicating the formation of the cationic alkyne complexes $[Cr(CO)_2(\eta\text{-}Me_3SiC{\equiv}CSiMe_3)(\eta\text{-arene})][PF_6]$ (arene = 1,2,3,5-$Me_4H_2C_6$ **2A**$^+$, 1,2,3-$Me_3H_3C_6$ **3A**$^+$ or C_6H_6 **4A**$^+$).

The chemical oxidation of the molybdenum complexes **5V** and **6V** was carried out in a similar manner to that of the chromium complexes **2V**–**4V**, reaction with one equivalent of $[Fe(\eta\text{-}C_5H_5)_2][PF_6]$ resulting in an immediate colour change from orange to pale yellow. With **5V**, the IR spectrum showed two new carbonyl bands at 2001 and 1941 cm^{-1} and a weak ν(C≡C) band at 1736 cm^{-1} consistent with the formation of the cationic alkyne complex $[Mo(CO)_2(\eta\text{-}Me_3SiC{\equiv}CSiMe_3)(\eta\text{-}C_6Me_6)]^+$ **5A**$^+$. However, the oxidation of **6V** did not proceed as cleanly and the IR spectrum of the product solution contained five peaks, at 2050, 2013, 1988, 1957 and 1895 cm^{-1}. The strongest two peaks, at 2013 and 1957 cm^{-1}, are assigned to ν(CO) for the alkyne complex $[Mo(CO)_2(\eta\text{-}Me_3SiC{\equiv}CSiMe_3)(\eta\text{-}C_6H_3Me_3\text{-}1,3,5)][PF_6]$ **6A**$^+$ by comparison with those of **5A**$^+$ but the other peaks remain unidentified. Attempts to isolate **2A**$^+$–**6A**$^+$ were unsuccessful; their stability decreases with decreasing methylation of the arene and, more strikingly, on changing the metal from chromium to molybdenum.

In order to study the stability of the neutral alkyne complexes **2A**–**6A**, solutions of the cations **2A**$^+$–**6A**$^+$ were generated at 0 °C from the neutral vinylidene complexes **2V**–**6V** as described above. Addition of one equivalent of the mild reducing agent $[NBu^n_4][BH_4]$ then resulted in an immediate colour change from yellow to orange. The IR spectrum of each solution showed four new carbonyl bands at lower energy than those of **2A**$^+$–**6A**$^+$. Two of the bands correspond to those of the neutral vinylidene complexes **2V**–**4V**. The other peaks, at slightly lower energy (*ca.* 25 cm^{-1}) than those of the vinylidene complex, are assigned to the neutral alkyne complexes $[Cr(CO)_2(\eta\text{-}Me_3SiC{\equiv}CSiMe_3)(\eta\text{-arene})]$ (arene = $C_6H_2Me_4$-1,2,3,5 **2A**, $C_6H_3Me_3$-1,2,3 **3A** or C_6H_6 **4A**). Over *ca.* 20 min the peaks due to the alkyne complexes **2A**–**4A** are replaced by those of the corresponding vinylidene complexes as the alkyne-to-vinylidene isomerisation slowly occurs.

The reduction of the molybdenum complex **5A**$^+$ with one equivalent of $[Co(\eta\text{-}C_5H_5)_2]$ gave an immediate colour change from yellow to orange, the resulting solution showing only two IR carbonyl bands, at 1879 and 1802 cm^{-1}, assigned to the alkyne complex $[Mo(CO)_2(\eta\text{-}Me_3SiC{\equiv}CSiMe_3)(\eta\text{-}C_6Me_6)]$ **5A**. These bands were then replaced by those of the neutral vinylidene complex **5V** over the next hour. Although the oxidation of $[Mo(CO)_2\{C{=}C(SiMe_3)_2\}(\eta\text{-}C_6H_3Me_3\text{-}1,3,5)]$ **6V** with $[Fe(\eta\text{-}C_5H_5)_2][PF_6]$ does not proceed cleanly, as noted above, addition of approximately one equivalent of $[Co(\eta\text{-}C_5H_5)_2]$ to the reaction mixture resulted in the replacement of the carbonyl bands assigned to **6A**$^+$ by four bands which can be assigned to the neutral alkyne complex **6A** and the vinylidene complex **6V**.

The oxidation and reduction sequences described above are similar to those observed for $[Cr(CO)_2\{C{=}C(SiMe_3)_2\}(\eta\text{-}C_6Me_6)]$ **1V** and likewise can be represented by a square scheme (Scheme 1). The qualitative chemical oxidation and reduction studies noted above allow the identification of three members of the square scheme (the vinylidene cations have not been detected by IR spectroscopy, but their ESR spectra are described below). Moreover, it is clear that isomerisation of the neutral alkyne complexes to the vinylidene isomers is much slower than that of the cationic vinylidene to the alkyne containing cation. This has been quantified for **1V**[1] but the present qualitative study suggests that alkyne-to-vinylidene isomerisation is slower for the d^6 molybdenum complexes **5A** and **6A** than for the chromium complexes **2A**–**4A**.

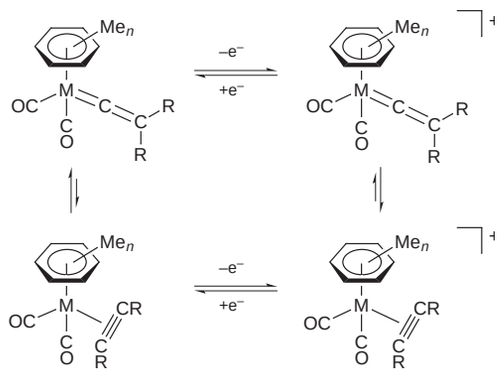

Scheme 1 Square scheme for redox-induced vinylidene–alkyne isomerisations.

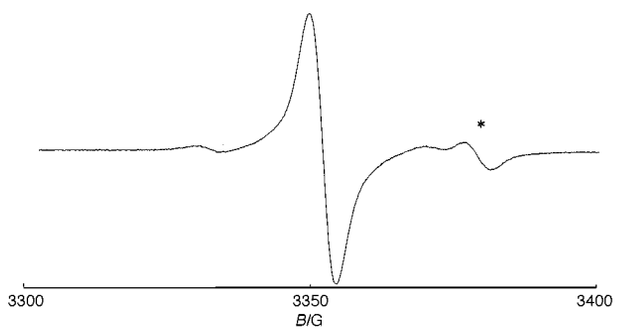

Fig. 5 The ESR spectrum of $[Cr(CO)_2\{C{=}C(SiMe_3)_2\}(\eta\text{-}C_6H_6)]^+$ **4V**$^+$ in CH_2Cl_2 at 190 K. The asterisk (*) marks the spectrum of $[Cr(CO)_2(\eta\text{-}Me_3SiC{\equiv}CSiMe_3)(\eta\text{-}C_6H_6)]^+$ **4A**$^+$.

ESR spectroscopic studies of the paramagnetic vinylidene and alkyne complex cations

The electronic structures of the paramagnetic vinylidene and alkyne complexes described above have been probed by ESR spectroscopy. At low temperatures the vinylidene-to-alkyne isomerisation is retarded and the cationic vinylidene complexes $[M(CO)_2\{C{=}C(SiMe_3)_2\}(\eta\text{-arene})]^+$ can be detected by ESR spectroscopy.

The complexes **2V**$^+$–**6V**$^+$ were generated *in situ* by adding solid $[Fe(\eta\text{-}C_5H_5)_2][PF_6]$ to frozen CH_2Cl_2 solutions of **2V**–**6V** at 77 K. The frozen solution was transferred to the cavity of the ESR spectrometer and allowed to warm to 190 K; after *ca.* 10 min, a spectrum assignable to the vinylidene cation was observed. These spectra consist of a relatively broad line, $\langle g\rangle \approx 2.014$–2.015, usually accompanied by one or more satellites assigned to coupling to ^{53}Cr (I = 3/2, 9.5% abundance) or $^{95,97}Mo$ (I = 5/2, 25.5% abundance). A sharper line, also accompanied by satellites, is observed at higher field and assigned to the alkyne complex, $[M(CO)_2(\eta\text{-}Me_3SiC{\equiv}CSiMe_3)(\eta\text{-arene})]^+$ **2A**$^+$–**6A**$^+$. (Fig. 5 shows the ESR spectrum of **4V**$^+$ accompanied by a small amount of **4A**$^+$.) At 190 K, the alkyne lines are much weaker than those assigned to the vinylidene complex, but at higher temperatures, they increase in intensity at the expense of the vinylidene lines, and at 250 K or above, only the spectrum of the alkyne complex is observed. ESR parameters for **1V**$^+$–**6V**$^+$ and **1A**$^+$–**6A**$^+$ are given in Table 5. For comparison, parameters for $[Cr(CO)_2(\eta\text{-}RC{\equiv}CR')(\eta\text{-}C_6Me_6)]^+$ (R = R′ = CO_2Et **7A**$^+$, C_6H_4OMe-4 **8A**$^+$; R = Ph, R′ = H **9A**$^+$),[2] generated directly from the neutral alkyne complexes **7A**–**9A** by oxidation with $[Fe(\eta\text{-}C_5H_5)_2][PF_6]$, are given in Table 6, and g components, measured from frozen CH_2Cl_2–thf solution spectra of **1V**$^+$,[1] **1A**$^+$, **7A**$^+$[2] and **8A**$^+$, are given in Table 7.

The ^{53}Cr or $^{95,97}Mo$ satellites observed in the spectra of **1A**$^+$–**9A**$^+$ exhibit a dependence of line width on m_I, the nuclear spin quantum number, with the high-field lines substantially broader than those at low field. The lowest-field feature is usually

Table 5 Isotropic ESR parameters for $[M(CO)_2\{C{=}C(SiMe_3)_2\}(\eta\text{-arene})]^+$ and $[M(CO)_2(\eta\text{-}Me_3SiC{=}CSiMe_3)(\eta\text{-arene})]^+$ in CH_2Cl_2

M	arene	Complex	$\langle g\rangle$	$\langle a^M\rangle$/G	Complex	$\langle g\rangle$	$\langle a^M\rangle$/G	$\langle a^H\rangle$/G
Cr	C_6Me_6	**1V**$^+$ [a]	2.0139(2)	13.1(1)	**1A**$^+$	1.9983(1)	16.77(1)	—
Cr	$C_6H_2Me_4$-1,2,3,5	**2V**$^+$	2.0155(2)	12.8(1)	**2A**$^+$	1.9991(1)	16.8(3)	1.50(5) (2 H)
Cr	$C_6H_3Me_3$-1,3,5	**3V**$^+$	2.0150(1)	13.15(3)	**3A**$^+$	1.9989(1)	16.79(2)	—
Cr	C_6H_6	**4V**$^+$	2.0140(2)	13.09(6)	**4A**$^+$	1.9980(1)	17.02(1)	1.418(5) (6 H)
Mo	C_6Me_6	**5V**$^+$	2.0412(1)	18.1(3)	**5A**$^+$	2.0140(1)	29.65(3)	—
Mo	$C_6H_3Me_3$-1,3,5	**6V**$^+$	2.0436(6)	18.5(4)	**6A**$^+$	2.0160(1)	29.74(4)	2.2(1) (3 H)

[a] From ref. 1.

Table 6 Isotropic ESR parameters for $[Cr(CO)_2(\eta\text{-}RC{\equiv}CR')(\eta\text{-}C_6Me_6)]^+$ in CH_2Cl_2

Complex	R	R′	$\langle g\rangle$	$\langle a^{Cr}\rangle$/G	$\langle a^X\rangle$/G
7A$^+$ [a]	CO_2Et	CO_2Et	1.9936(1)	16.78(3)	9.1(1) (2 C)
8A$^+$	C_6H_4-OMe-4	C_6H_4-OMe-4	1.9956(1)	14.38(2)	—
9A$^+$	Ph	H	1.9964(1)	16.12(2)	4.17(5) (1 H)

[a] From ref. 2.

Table 7 Anisotropic ESR parameters for arene metal complexes

Complex	g_x	g_y	g_z	Ref.
$[Cr(\eta\text{-}C_6H_6)_2]^+$	1.978	1.978	2.002	19
$[Mo(\eta\text{-}C_6H_6)_2]^+$	1.977	1.977	1.998	20
1V$^+$	1.993	2.020	2.030	1
1A$^+$	1.994	1.986	2.017	This work
7A$^+$	1.995	1.979	2.007	2
8A$^+$	1.996	1.983	2.009	This work

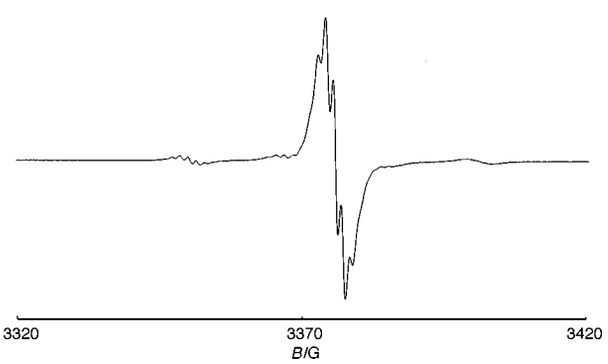

Fig. 6 The ESR spectrum of $[Cr(CO)_2(\eta\text{-}Me_3SiC{\equiv}CSiMe_3)(\eta\text{-}C_6H_6)]^+$ **4A**$^+$ in CH_2Cl_2 at 250 K, showing hyperfine coupling to the arene protons and the variation in line width of the ^{53}Cr satellites.

sharper than the central line and, in some spectra of alkyne complexes, *e.g.* that of $[Cr(CO)_2(\eta\text{-}Me_3SiC{\equiv}CSiMe_3)(\eta\text{-}C_6H_6)]^+$ **4A**$^+$ (Fig. 6), arene proton hyperfine coupling is resolved comparable to that observed in the spectra of the sandwich complexes $[M(\eta\text{-arene})_2]^+$ (M = Cr, Mo),[19,20] anisotropic ESR parameters for which are given in Table 7.

Extended Hückel MO calculations were performed on $[Cr(\eta\text{-}C_6H_6)_2]^+$, $[Cr(CO)_2(\eta\text{-}HC{\equiv}CH)(\eta\text{-}C_6H_6)]^+$, and $[Cr(CO)_2(C{=}CH_2)(\eta\text{-}C_6H_6)]^+$ using idealised coordinates derived from the crystal structures of the Cr(0) complexes $[Cr(\eta\text{-}C_6H_6)_2]$,[21] $[Cr(CO)_2(\eta\text{-}PhC{\equiv}CPh)(\eta\text{-}C_6Me_5H)]$[4] and **4V** respectively, and parameters collated by Alvarez.[22] The results for $[Cr(\eta\text{-}C_6H_6)_2]^+$ are essentially identical to those reported by Muetterties *et al.*[23] The a_{1g} SOMO is nearly purely metal d_{z^2}, and the e_{2g} pair, largely metal $d_{x^2-y^2}$ and d_{xy}, lies at slightly lower energy. Metal d_{xz} and d_{yz} mainly contribute to weakly anti-bonding, empty MOs. The frontier orbitals for the alkyne and vinylidene complexes show family resemblances to those of $[Cr(\eta\text{-}C_6H_6)_2]^+$ although the lower symmetry allows considerable d-orbital hybridisation; the principal interactions for the $Cr(CO)_2(\eta\text{-}C_6H_6)$ vinylidene complex are similar to those shown in Fig. 2 for the isoelectronic $[Mn(CO)_2(\eta\text{-}C_5H_5)]^+$ fragment. For both the alkyne and vinylidene complexes, the a′ SOMO is significantly delocalised into ligand π orbitals and the metal contribution is a $d_{z^2}/d_{x^2-y^2}/d_{xz}$ hybrid: 28, 12 and 2% for the vinylidene complex, 43, 11 and 0.3% for the alkyne complex; in either case, the metal contribution is best described as $d_{z^2-x^2}$. The next two filled MOs, related to the e_{2g} pair for $[Cr(\eta\text{-}C_6H_6)_2]^+$, are an a′ MO with metal $d_{x^2-y^2}/d_{z^2}/d_{xz}$ character (34, 16 and 3% for the vinylidene complex, 44, 11 and 0.4% for the alkyne complex, in either case best described as d_{y^2}) and an a″ MO with metal d_{xy}/d_{yz} character (44 and 2% for the vinylidene complex, 45 and 6% for the alkyne complex), similar to the a″ orbital of Fig. 2. These orbitals are very similar in shape to those found by Hoffmann[14] for $[Mn(CO)_2(HC{\equiv}CH)(\eta\text{-}C_5H_5)]$ and $[Mn(CO)_2(C{=}CH_2)(\eta\text{-}C_5H_5)]$, but the energy order of the two a′ molecular orbitals is inverted.

The d_{z^2} character of the SOMO is confirmed for the alkyne complexes by the appearance of hyperfine coupling to the arene ring protons. The proton couplings observed in the ESR spectra of $[Cr(\eta\text{-}C_6H_6)_2]^+$ (3.46 G),[19] $[Mo(\eta\text{-}C_6H_6)_2]^+$ (4.45 G),[20] and related species are positive in sign[24] and have been interpreted as resulting from direct delocalisation of the predominantly metal d_{z^2} SOMO into the σ-orbitals of the arene;[25] the usual mechanism whereby proton couplings in arene radical ions arise from spin polarisation by π spin density is of negligible importance in these systems. If we assume that the arene proton coupling is proportional to the metal d_{z^2} character, the observed 3.46 G coupling for $[Cr(\eta\text{-}C_6H_6)_2]^+$, together with the EHMO calculations, suggests a coupling of 1.6 G for $[Cr(CO)_2(\eta\text{-}HC{\equiv}CH)(\eta\text{-}C_6H_6)]^+$ and 1.4 G for $[Cr(CO)_2(C{=}CH_2)(\eta\text{-}C_6H_6)]^+$. This prediction is in reasonable agreement with the observed couplings for **2A**$^+$ and **4A**$^+$. No proton coupling could be resolved for the vinylidene complexes, in part because the isotropic spectra could be observed only at relatively low temperatures where lines are too broad to resolve the proton coupling. The larger proton coupling found for **6A**$^+$ is consistent with the larger coupling observed for $[Mo(\eta\text{-}C_6H_6)_2]^+$.

Spin–orbit coupling of the d_{z^2} SOMO with d_{xz} and d_{yz} for $[Cr(\eta\text{-}C_6H_6)_2]^+$ leads to $g_\perp < g_e$, $g_\parallel = g_e$. In addition to similar contributions for the alkyne and vinylidene model complexes, coupling of the $d_{x^2-y^2}$ SOMO contribution with d_{xy} leads to g_z slightly larger than the free-electron value. For the alkyne complex, the d_{xz} contributions to empty MOs still dominate so that g_y remains less than g_e, but for the vinylidene complex, the d_{xz} contributions to the SOMO and to the filled MOs lead to g_y slightly larger than g_e. In general, these results are in good agreement with the experimental results and allow us to make tentative assignments of the *g*-matrix components: for the alkyne complexes, $g_z > g_x > g_y$; for the vinylidene complexes, $g_z > g_y > g_x$.

The m_I-dependence of the satellite line widths is similar to that observed in the spectra of $[Cr(\eta\text{-}C_6H_6)_2]^+$ and related species.[26] Line widths can be expressed by eqn. (1) where

$$\text{Width} = \alpha + \beta m_I + \gamma m_I^2 \qquad (1)$$

the parameters α, β and γ are related to the anisotropies of the

g- and metal-hyperfine matrices.[27] In the case of $[Cr(\eta\text{-}C_6H_6)_2]^+$, it is known that $\langle a^{Cr}\rangle$ is positive so that the observed increase in width with increasing magnetic field implies that β is negative. (The nuclear magnetic moments of ^{53}Cr and $^{95,97}Mo$ are negative so that a spin polarisation mechanism is expected to lead to positive isotropic coupling constants.) For $\omega_0\tau_r \gg 1$, $|\langle A\rangle|/\omega_0 \ll 1$, the parameter β is given by eqn. (2), where τ_r is the

$$\beta = \tfrac{4}{15} B_0(b\,\Delta\gamma + 4c\,\delta\gamma)\,\tau_r \qquad (2)$$

rotational correlation time, ω_0 is the angular microwave frequency, and the other parameters are given by eqns. (3a–d). For

$$b = \tfrac{2}{3}[A_z - \tfrac{1}{2}(A_x + A_y)] \qquad (3a)$$

$$c = \tfrac{1}{4}(A_x - A_y) \qquad (3b)$$

$$\Delta\gamma = \frac{2\pi\mu_B}{h}[g_z - \tfrac{1}{2}(g_x + g_y)] \qquad (3c)$$

$$\delta\gamma = \frac{\pi\mu_B}{h}(g_x - g_y) \qquad (3d)$$

$[Cr(\eta\text{-}C_6H_6)_2]^+$, $c = \delta\gamma = 0$, $\Delta\gamma > 0$ and, for the d_{z^2} SOMO, we expect A_z, and thus b, to be negative, consistent with the observed line widths. Assuming $\langle A^{Cr}\rangle$ is also positive for the alkyne and vinylidene cations, we again have $\beta < 0$. With the *g*-component assignments given in Table 7, $\Delta\gamma > 0$ for both alkyne and vinylidene complexes, $\delta\gamma > 0$ for alkyne complexes, and $\delta\gamma < 0$ for vinylidene complexes. If we describe the metal SOMO contribution as $d_{z^2-x^2}$, we expect a dipolar contribution $+Q$ to A_y, $-Q/2$ to A_x and A_z; thus $b = -Q/2$, $c = -3Q/8$. Substituting numbers in eqn. (3c), (3d) and (2), we find $\beta_{alkyne} \ll \beta_{vinylidene} < 0$, consistent with the experimental results.

Coupling to a single proton was observed in the ESR spectrum of $[Cr(CO)_2(\eta\text{-}PhC{\equiv}CH)(\eta\text{-}C_6Me_6)]^+$ **9A**$^+$ [2] and to two ^{13}C nuclei in the spectrum of $[Cr(CO)_2(EtCO_2C{\equiv}CCO_2Et)(\eta\text{-}C_6Me_6)]^+$ **7A**$^+$. Lines in the spectra of $[Cr(CO)_2(\eta\text{-}4\text{-}MeOC_6H_4C{\equiv}CC_6H_4OMe\text{-}4)(\eta\text{-}C_6Me_6)]^+$ **8A**$^+$ are significantly broader than those of **7A**$^+$ and are noticeably non-Lorentzian, suggesting unresolved hyperfine coupling to the phenyl ring protons. These results are consistent with the extensive delocalisation of the SOMO into the alkyne π-orbitals predicted by EHMO calculations. Indeed, the EHMO results suggest a carbon $2p_\pi$ spin density of 0.074, nearly large enough to explain the proton coupling for **9A**$^+$ in terms of the usual indirect polarisation mechanism.

Since the ^{53}Cr or $^{95,97}Mo$ couplings arise primarily through polarisation of inner-shell s-orbitals by 3d or 4d metal spin density, it is tempting to use these couplings as measures of the metal d-orbital character in the SOMOs. Since $\langle a^{Cr}\rangle = 18.1$ G for $[Cr(\eta\text{-}C_6H_6)_2]^+$,[19] this measure would suggest a SOMO with nearly as much Cr 3d character for the alkyne complexes and only slightly smaller values for the vinylidene complexes. Unfortunately, in all cases the SOMOs belong to totally symmetric representations and metal 4s character is permitted. This leads to a negative contribution to $\langle a^{Cr}\rangle$, $-267\,\rho_{4s}$ G,[28] cancelling part of the dominant polarisation contribution. EHMO calculations suggest that metal 4s SOMO character is sufficiently variable that the metal coupling cannot be used as a reliable measure of metal 3d SOMO character.

Conclusions

UV irradiation of $[M(CO)_3(\eta\text{-}C_6Me_{6-n}H_n)]$ (M = Cr, Mo) with the alkyne $Me_3SiC{\equiv}CSiMe_3$ generally gives the vinylidene complexes $[M(CO)_2\{C{=}C(SiMe_3)_2\}(\eta\text{-}C_6H_nMe_{6-n})]$ rather than the alkyne complexes $[M(CO)_2(\eta\text{-}Me_3SiC{\equiv}CSiMe_3)(\eta\text{-}C_6H_nMe_{6-n})]$. However, the molybdenum complex $[Mo(CO)_2\{C{=}C(SiMe_3)_2\}(\eta\text{-}C_6H_3Me_3\text{-}1,3,5)]$ reaches thermal equilibrium with the alkyne complex $[Mo(CO)_2(\eta\text{-}Me_3SiC{\equiv}CSiMe_3)(\eta\text{-}C_6H_3Me_3\text{-}1,3,5)]$ in solution. By contrast, for the more substituted arene complexes such as $[Mo(CO)_2\{C{=}C(SiMe_3)_2\}(\eta\text{-}C_6Me_6)]$, no vinylidene-to-alkyne isomerisation is observed.

One-electron oxidation of the vinylidene complexes $[M(CO)_2\{C{=}C(SiMe_3)_2\}(\eta\text{-}C_6H_nMe_{6-n})]$ (M = Mo, Cr) gives the cationic alkyne complexes $[M(CO)_2(\eta\text{-}Me_3SiC{\equiv}CSiMe_3)(\eta\text{-}C_6H_nMe_{6-n})]^+$ *via* a fast redox-induced vinylidene-to-alkyne isomerisation. However, on reduction the neutral alkyne complex $[M(CO)_2\{C{=}C(SiMe_3)_2\}(\eta\text{-}C_6H_nMe_{6-n})]$ is formed which slowly isomerises to the neutral vinylidene complex.

Analysis of the ESR spectra of $[M(CO)_2\{C{=}C(SiMe_3)_2\}(\eta\text{-}C_6H_nMe_{6-n})]^+$ and $[M(CO)_2(\eta\text{-}Me_3SiC{\equiv}CSiMe_3)(\eta\text{-}C_6H_nMe_{6-n})]^+$ shows the unpaired electron to be extensively delocalised on to the alkyne, in agreement with the results of EHMO calculations.

Experimental

The preparation, purification and reactions of the complexes described were carried out under an atmosphere of dry dinitrogen using dried, distilled and deoxygenated solvents; reactions were monitored by IR spectroscopy where necessary. The compounds $[M(CO)_3(\eta\text{-arene})]$ (M = Cr[29] or Mo[30]), $[Cr(CO)_2\{C{=}C(SiMe_3)_2\}(\eta\text{-}C_6Me_6)]$,[1] $[Cr(CO)_2(\eta\text{-}RC{\equiv}CR')(\eta\text{-}C_6Me_6)]$ (R = R′ = Ph, 4-$MeOC_6H_4C{\equiv}CC_6H_4OMe$-4, CO_2Et; R = Ph, R′ = H)[3] and $[Fe(\eta\text{-}C_5H_5)_2][PF_6]$[31] were prepared by published methods. IR spectra were recorded on a Nicolet 5ZDX FT spectrometer. ^1H and ^{13}C NMR spectra were recorded on JEOL GX270, λ300 or GX400 spectrometers with $SiMe_4$ as internal standard. X-Band ESR spectra were recorded using a Bruker ESP-300E spectrometer equipped with a Bruker variable-temperature accessory and a Hewlett Packard 5350B microwave frequency counter. The field calibration was checked by measuring the resonance of the diphenylpicrylhydrazyl (dpph) radical. Cyclic voltammetry was carried out as previously described;[32] for rpev the platinum electrode was rotated at 600 r.p.m. Under the conditions used for voltammetry, $E^{\circ\prime}$ for the one-electron reduction of $[Co(\eta\text{-}C_5H_5)_2][BF_4]$, added to the test solutions as an internal calibrant, is −0.87 V. (On this scale, the one-electron oxidation of ferrocene occurs at 0.47 V.) Microanalyses were carried out by the staff of the Microanalytical Service of the School of Chemistry, University of Bristol.

Syntheses

$[Cr(CO)_2\{C{=}C(SiMe_3)_2\}(\eta\text{-}C_6H_2Me_4\text{-}1,2,3,5)]$ 2V. A stirred solution of $[Cr(CO)_3(\eta\text{-}C_6H_2Me_4\text{-}1,2,3,5)]$ (0.50 g, 1.85 mmol) and $Me_3SiC{\equiv}CSiMe_3$ (2 cm^3, 8.90 mmol) in thf (70 cm^3) was irradiated under UV light for 5 h while a slow purge of nitrogen (*ca.* 1 bubble per second) was passed through the mixture. The resulting brown-orange solution was evaporated to dryness *in vacuo* and the residue extracted into *n*-hexane (70 cm^3). After filtration through Celite, the orange solution was reduced in volume to *ca.* 20 cm^3 and then stored at −20 °C for 18 h giving the product as orange needles, yield 0.30 g (39%). The solid complex is stable in air for several weeks. It dissolves in most organic solvents to give moderately air-sensitive solutions.

The complexes $[Cr(CO)_2\{C{=}C(SiMe_3)_2\}(\eta\text{-}C_6H_3Me_3\text{-}1,2,3)]$ **3V** and $[Cr(CO)_2\{C{=}C(SiMe_3)_2\}(\eta\text{-}C_6H_6)]$ **4V** were prepared similarly; UV irradiation was carried out in *n*-hexane (for 6 h and 27 h respectively) and the reaction mixture was filtered, evaporated to low volume *in vacuo* and cooled to induce crystallisation. Air stability, both in the solid state and in solution, decreases with decreasing methylation of the arene ligand.

$[Mo(CO)_2\{C{=}C(SiMe_3)_2\}(\eta\text{-}C_6Me_6)]$ 5V. A stirred solution of $[Mo(CO)_3(\eta\text{-}C_6Me_6)]$ (0.50 g, 1.46 mmol) and $Me_3SiC{\equiv}CSiMe_3$ (2 cm^3, 8.90 mmol) in benzene (120 cm^3), purged with a stream of N_2, was irradiated under UV light for 16 h to give an

Table 8 Crystal and refinement data for complex **4V**

Formula	$C_{16}H_{24}CrO_2Si_2$
M	356.53
Crystal system	Monoclinic
Space group (no.)	$C2/c$ (15)
a/Å	34.627(7)
b/Å	6.8137(14)
c/Å	16.501(3)
β/°	94.67(3)
T/K	293(2)
U/Å^3	3880.3(14)
Z	8
μ/mm^{-1}	0.714
Reflections collected	3441
Independent reflections (R_{int})	3373 (0.0468)
Goodness-of-fit on F^2	1.138
Final R indices [$I > 2\sigma(I)$]: $R1$, $wR2$	0.0662, 0.1419

orange solution which was evaporated to dryness *in vacuo*. The residue was extracted into diethyl ether (180 cm^3) and filtered through Celite to give an orange solution which was treated with *n*-hexane (80 cm^3). Removal of the diethyl ether *in vacuo* and cooling to −20 °C for 5 h gave the product as orange needles, yield 0.19 g (27%). The solid complex is stable in air for *ca*. 1 d and soluble in most organic solvents (sparingly in *n*-hexane, insoluble in MeCN) to give solutions which decompose in air in minutes.

The complex $[Mo(CO)_2\{C{=}C(SiMe_3)_2\}(\eta\text{-}C_6H_3Me_3\text{-}1,3,5)]$ **6V** was prepared similarly, in *n*-hexane. The reaction mixture also contains small amounts of $[Mo(CO)_2(\eta\text{-}Me_3SiC{\equiv}CSiMe_3)(\eta\text{-}C_6H_3Me_3\text{-}1,3,5)]$ but crystallisation of the filtered solution at −20 °C gave pure orange-red needles of $[Mo(CO)_2\{C{=}C(SiMe_3)_2\}(\eta\text{-}C_6H_3Me_3\text{-}1,3,5)]$. The solid is stable in air for a few hours; solutions in organic solvents are air-sensitive.

Structure determination of $[Cr(CO)_2\{C{=}C(SiMe_3)_2\}(\eta\text{-}C_6H_6)]$ 4V

Many of the details of the structure analysis of $[Cr(CO)_2\{C{=}C(SiMe_3)_2\}(\eta\text{-}C_6H_6)]$ **4V** are presented in Table 8. Crystal decay of *ca*. 35% was observed over the period of data collection; an appropriate correction was made.

CCDC reference number 186/1336.

Acknowledgements

We thank the EPSRC for a Postdoctoral Research Associateship (to T. J. P.), the Spanish Ministerio de Educacion y Ciencia for an FPU (Becas en el extranjero) grant (to A. J. M.) and the University of Bristol for a Postgraduate Scholarship (to I. M. B.).

References

1 N. G. Connelly, W. E. Geiger, M. C. Lagunas, B. Metz, A. L. Rieger, P. H. Rieger and M. J. Shaw, *J. Am. Chem. Soc.*, 1995, **117**, 12202.
2 N. G. Connelly, A. G. Orpen, A. L. Rieger, P. H. Rieger, C. J. Scott and G. M. Rosair, *J. Chem. Soc., Chem. Commun.*, 1992, 1293.
3 N. G. Connelly and G. A. Johnson, *J. Organomet. Chem.*, 1974, **77**, 341.
4 I. M. Bartlett, N. G. Connelly, A. G. Orpen, M. J. Quayle and J. C. Rankin, *Chem. Commun.*, 1996, 2583.
5 R. Davis and L. A. P. Kane-Maguire, in *Comprehensive Organometallic Chemistry*, eds. G. W. Wilkinson, F. G. A. Stone and E. W. Abel, Pergamon Press, Oxford, 1982, vol. 3, 1035.
6 R. Davis and L. A. P. Kane-Maguire, in *Comprehensive Organometallic Chemistry*, eds. G. W. Wilkinson, F. G. A. Stone and E. W. Abel, Pergamon Press, Oxford, 1982, vol. 3, 1218.
7 M. I. Bruce, *Chem. Rev.*, 1991, **91**, 197.
8 M. I. Bruce and A. G. Swincer, *Adv. Organomet. Chem.*, 1983, **22**, 59.
9 A. B. Antonova, N. E. Kolobova, P. V. Petrovsky, B. V. Lokshin and N. S. Obezyuk, *J. Organomet. Chem.*, 1977, **137**, 55.
10 U. Schubert and J. Grönen, *Chem. Ber.*, 1989, **122**, 1237; U. Schubert, U. Kirchgässner, J. Grönen and H. Piana, *Polyhedron*, 1989, **8**, 1589.
11 P. D. Magnus, T. Sarkar and S. Djuric, in *Comprehensive Organometallic Chemistry*, eds. G. W. Wilkinson, F. G. A. Stone and E. W. Abel, Pergamon Press, Oxford, 1982, vol. 7, 515.
12 B. Rees and P. Coppens, *Acta Crystallogr., Sect. B*, 1973, **29**, 2516.
13 H. Berke, G. Huttner and J. von Seyerl, *J. Organomet. Chem.*, 1981, **218**, 193.
14 J. Silvestre and R. Hoffmann, *Helv. Chim. Acta*, 1985, **68**, 1461.
15 N. M. Kostic and R. F. Fenske, *Organometallics*, 1982, **1**, 974.
16 K. R. Birdwhistell, T. L. Tonker and J. L. Templeton, *J. Am. Chem. Soc.*, 1987, **109**, 1401.
17 R. M. Bullock, *J. Chem. Soc., Chem. Commun.*, 1989, 165.
18 J. J. Kowalczyk, A. M. Arif and J. A. Gladysz, *Organometallics*, 1991, **10**, 1079.
19 R. Prins and F. J. Reinders, *Chem. Phys. Lett.*, 1969, **3**, 45.
20 K. H. Hausser, *Naturwissenshaften*, 1961, **48**, 426.
21 E. Keules and F. Jellinek, *J. Organomet. Chem.*, 1966, **5**, 490.
22 S. Alvarez, *Tables of Parameters for Extended Huckel Calculations*, University of Barcelona, Barcelona, 1989.
23 E. L. Muetterties, J. R. Bleeke, E. J. Wucherer and T. A. Albright, *Chem. Rev.*, 1982, **82**, 499.
24 A. D. Krivospitskii and G. K. Chirkin, *Zh. Strukt. Khim.*, 1974, **15**, 25.
25 S. E. Anderson, Jr. and R. S. Drago, *Inorg Chem.*, 1972, **11**, 1564.
26 W. Karthe and W. Kleinwächter, *Ann. Phys.* (*Leipzig*), 1968, **21**, 137; B. G. Gribov, B. I. Kozyrkin, A. D. Krivospitskii and G. K. Chirkin, *Dokl. Akad. Nauk SSSR*, 1970, **193**, 91.
27 R. Wilson and D. Kivelson, *J. Chem. Phys.*, 1966, **44**, 4445.
28 J. R. Morton and K. F. Preston, *J. Magn. Reson.*, 1978, **30**, 577.
29 B. Nicholls and M. C. Whiting, *J. Chem. Soc.*, 1959, 551.
30 A. Pidcock, J. D. Smith and B. W. Taylor, *J. Chem. Soc. A*, 1967, 872.
31 N. G. Connelly and W. E. Geiger, *Chem. Rev.*, 1996, **96**, 877; J. C. Smart and B. L. Pinsky, *J. Am. Chem. Soc.*, 1980, **102**, 1009.
32 N. C. Brown, G. B. Carpenter, N. G. Connelly, J. G. Crossley, A. Martin, A. G. Orpen, A. L. Rieger, P. H. Rieger and G. H. Worth, *J. Chem. Soc., Dalton Trans.*, 1996, 3977.

Paper 8/09451I